



Synthesis, characterization, Hirshfeld surface and theoretical properties of $(C_7H_{10}N)_4[H_2P_2Mo_5O_{23}] \cdot H_2O$

ALI HARCHANI^{a,*}, MONIKA KUČERÁKOVÁ^b, MICHAL DUŠEK^b and AMOR HADDAD^a

^aLaboratoire de Matériaux, Cristallographie et de Thermodynamique, Appliquée. Université Tunis El Manar, Faculté de Sciences de Tunis. Université de Monastir, Faculté des Sciences Monastir, 5019 Monastir, Tunisia

^bInstitute of Physics ASCR, Na Slovance 2, 182 21 Praha 8, Czech Republic

E-mail: ali.harchani@gmail.com

MS received 1 June 2017; revised 30 July 2017; accepted 6 August 2017; published online 6 September 2017

Abstract. The reaction of molybdic acid, phosphoric acid and copper(II) sulfate pentahydrate with m-toluidine in aqueous solution at room temperature furnished a new diphosphopentamolybdate $(C_7H_{10}N)_4[H_2P_2Mo_5O_{23}] \cdot H_2O$ (**1**). A single-crystal X-ray diffraction study showed that the compound crystallizes in the triclinic crystal system with space group $P - 1$ and unit cell constants, $a = 12.833(3) \text{ \AA}$, $b = 13.9855(4) \text{ \AA}$, $c = 14.9446(4) \text{ \AA}$, $\alpha = 64.607(3)^\circ$, $\beta = 70.578(2)^\circ$, $\gamma = 65.713(3)^\circ$. The sample was also analyzed by energy dispersive spectroscopy (EDS), infrared spectroscopy (IR) and UV-visible spectroscopy. Using the refined atomic structure, Hirshfeld surface analysis and Semi-empirical calculations were performed to study the intermolecular interactions and calculate theoretical properties of **1**.

Keywords. Diphosphopentamolybdate; synthesis; crystal structure; physicochemical properties; theoretical study.

1. Introduction

Polyoxometalates (POMs)^{1–4} are clusters of metal oxide units, possessing a vast array of physicochemical properties, which have been studied in various fields such as medicine, energy storage, catalysis, magnetism, and electrochromic applications, to name just a few.⁵ There are four principal types of heteropolyanion structures: Lindqvist structure, Anderson structure, Keggin structure and Dawson structure. An important class of polyoxometalates and diphosphopentamolybdates (abbreviated as $\{P_2Mo_5\}$) called the Strandberg family is included in heteropolyanion family.

Recently a series of compounds based on diphosphopentamolybdate cluster $[P_2Mo_5O_{23}]^{6-}$ linked through organoamine bases has been reported, such as $(H_2bpp)_3[P_2Mo_5O_{23}] \cdot H_2O$,⁶ $[(C_4N_2H_{12})_3][P_2Mo_5O_{23}] \cdot H_2O$,⁷ $[(C_3N_2H_{12})_3][P_2Mo_5O_{23}] \cdot 4H_2O$ ⁷ and $(C_5H_7N_2)_6[P_2Mo_5O_{23}]$.⁸ $[(C_4H_{10}NO)_5][HP_2Mo_5O_{23}] \cdot 5H_2O$,⁹ $[(HMTA-Me)_2][H_4P_2Mo_5O_{23}] \cdot 6H_2O$,⁹ $(enH_2)_2 \cdot [H_2P_2Mo_5O_{23}]$,⁹ $(enH_2)_2(en)_{0.5}[H_2P_2Mo_5O_{23}] \cdot 9H_2O$,⁹ $(enH_2)(enH_2)$

$[H_2P_2Mo_5O_{23}] \cdot 3H_2O$.⁹ Using the theoretical calculations applied to the polyoxometalates, we can get an idea about interactions, energy, electronic properties and other characteristics of their structures.

In the majority of previous works, such theoretical studies were not systematically performed on diphosphopentamolybdates. That is, a large number of Strandberg structures were synthesized and characterized but not theoretically studied. Herein, we focus on the semi-empirical calculations employed to investigate this type of compounds. We report the synthesis and crystal structure of a new title compound **1**, study its non-bonding interactions with the help of Hirshfeld surfaces, and discuss the results of theoretical calculations.

2. Experimental and theoretical

2.1 Materials and measurements

For the title compound, all reagents were purchased commercially and used without further purification. Molybdic acid (85%), phosphoric acid (85%), copper(II) sulfate pentahydrate (99%) and m-toluidine (99%) were from

*For correspondence

Sigma-Aldrich (France). The infrared spectrum of **1** was recorded at room temperature on a Perkin-Elmer Spectrometer (Tow ATR-FTIR) between 4000 and 400 cm^{-1} . A Perkin-Elmer Lambda-19 spectrophotometer was used to measure UV-Vis spectra in the 200–800 nm range using aqueous solutions. The energy dispersive analysis was performed using the Electron microscope FEI Quanta 200 model coupled to an X-ray energy dispersion analysis spectrometer.

2.2 Synthesis

The compound **1** was obtained by mixing molybdic acid (4 mmol, 0.648 g), phosphoric acid 85% (0.75 mL), copper(II) sulfate pentahydrate (0.5 mmol, 0.125 g) and H_2O (40 mL) in the first step. After stirring the mixture for 25 min at room temperature, m-toluidine (0.3 mL) was added. All reagents were stirred for 20 min at 70°C. The solution was then filtered and let at room temperature for several days to grow colorless crystals by slow evaporation. The EDS spectrum confirmed the presence of the Mo, P, O, N and C atoms (Figure 1).

2.3 X-ray crystallography

A single crystal of **1** of size $0.23 \times 0.13 \times 0.07 \text{ mm}^3$ was used for X-ray diffraction study at 120 K on Xcalibur, AtlasS2, Gemini Ultra diffractometer with mirrors-collimated, Cu K α radiation ($\lambda = 1.54184 \text{ \AA}$). The crystal structure was solved by charge flipping with program Superflip¹⁰ and refined with the Jana2006 program package.¹¹ In the structure of **1**, one disordered m-toluidine was refined in two distinct positions occupied 0.695(14):0.305(14), using the rigid body approach available in Jana2006.

The hydrogen atoms bonded to N and O atoms were found in difference Fourier map and refined with distance restraints. All other H atoms were kept in the geometrically correct positions with C—H distance of 0.96 \AA . The molecular structure plot was generated using Diamond 3.¹² The crystallographic data and structure refinements are summarized in Table 1.

2.4 Computational details

The semi-empirical calculations for **1** have been performed by the Spartan 14 V1.1.4 Wavefunction molecular modeling suite on a personal computer¹³ using PM6 semi-empirical model. The PM3 and PM6 semiempirical models were parameterized for most transition metals, and they usually provided good results.¹³ Hirshfeld surfaces computational analysis and associated 2D fingerprint plots¹⁴ were carried out using the Crystal Explorer 3.1 software¹⁵ and TONTO¹⁶ system.

3. Results and Discussion

3.1 Description of the crystal structure

The crystal structure of **1** (Figure 2) is built up of one symmetry-independent $[\text{H}_2\text{P}_2\text{Mo}_5\text{O}_{23}]^{4-}$ anion, four $(\text{C}_7\text{H}_{10}\text{N})^+$ cations and a molecule of water. The polyanion $[\text{H}_2\text{P}_2\text{Mo}_5\text{O}_{23}]^{4-}$ contains five distorted edge- and corner-sharing $[\text{MoO}_6]$ octahedra, and it is capped on both poles by two phosphatetetrahedra, each sharing three oxygen atoms with the molybdate ring. As shown in Figure 3, each $[\text{H}_2\text{P}_2\text{Mo}_5\text{O}_{23}]^{4-}$ anion is joined with two adjacent polyanions by strong hydrogen contacts of the type $\text{O}-\text{H} \cdots \text{O}$ ($\text{O}12 \cdots \text{O}19 = 2.695(7) \text{ \AA}$, $\text{O}24 \cdots \text{O}8 = 2.621(4) \text{ \AA}$) resulting in an infinite chain. This chains link each other through hydrogen bonds to generate a 2D network.

The Mo atoms are hexacoordinated with Mo—O distances in the range 1.688(4)–2.424(4) \AA and the O—Mo—O bond angles in the range 69.56(2)–173.99(3)°. Each $[\text{MoO}_6]$ octahedron in the structure has four bridging oxygen atoms and two terminal oxygen atoms. The P—O distances are in the range 1.517(3)–1.564(11) \AA and O—P—O bond angles are in the range 105.14(5)–113.20(9)°.

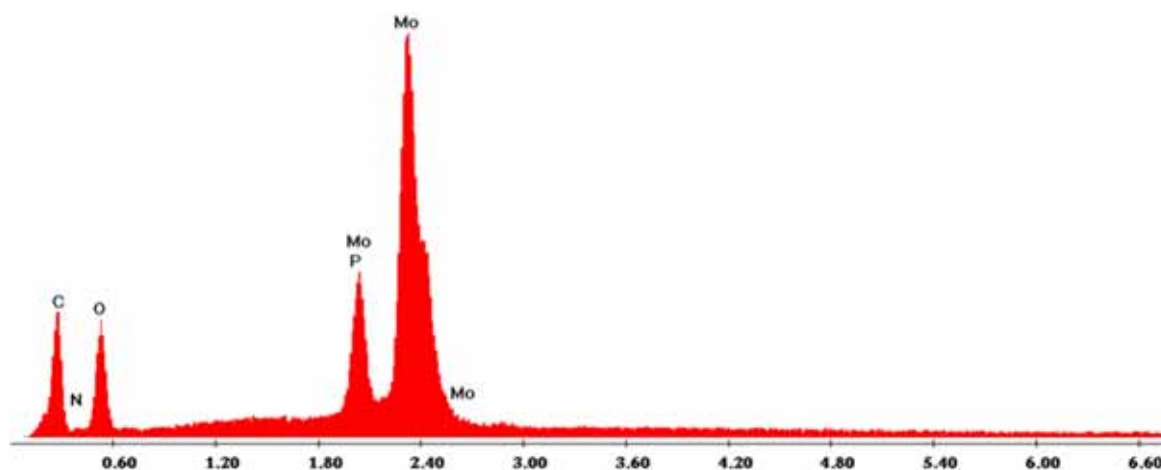
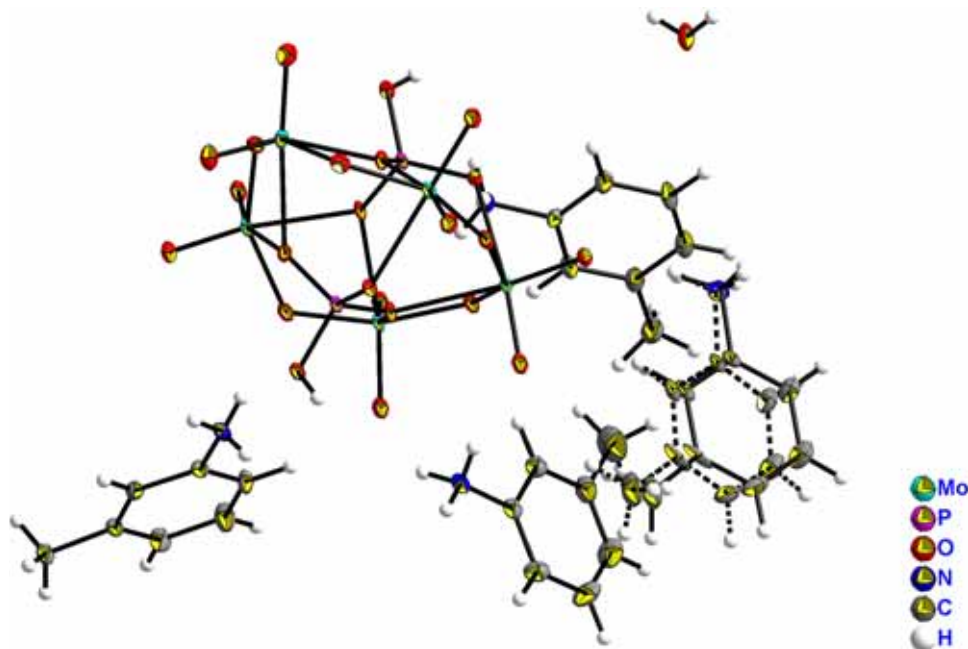


Figure 1. EDS pattern of $(\text{C}_7\text{H}_{10}\text{N})_4 [\text{H}_2\text{P}_2\text{Mo}_5\text{O}_{23}] \cdot \text{H}_2\text{O}$.

Table 1. Crystallographic data and structure refinements.

Formula	(C ₇ H ₁₀ N) ₄ [H ₂ P ₂ Mo ₅ O ₂₃] · H ₂ O
Formula weight (g mol ⁻¹)	1362.3
Temperature (K)	120
Wavelength (Å)	1.54184
Space group	P-1
Unit cell dimensions	
a (Å)	12.833 (3)
b (Å)	13.9855 (4)
c (Å)	14.9446 (4)
α (°)	64.607 (3)
β (°)	70.578 (2)
γ (°)	65.713 (3)
Cell volume (Å ³)	2165.21 (12)
Z	2
Absorption coefficient (mm ⁻¹)	13.05
Crystal size (mm ³)	0.234 × 0.130 × 0.066
Absorption correction	Multi-scan: T _{min} = 0.172, T _{max} = 1
Measured reflections	33625
Independent reflections	7758
Data/restraints/parameters	7758 /0/625
Goodness-of-fit	1.76
Weighting scheme	w = 1/(σ ² (F) + 0.0001F ²)
Final indices R[F ² > 3σ(F ²)], wR(F ²)	R ₁ = 0.0274, wR ₂ = 0.0369
R indices (all data)	R ₁ = 0.0320, wR ₂ = 0.0399
Δρ _{max} /Δρ _{min} (e.Å ⁻³)	1.47 /-0.83

**Figure 2.** View of the structure of compound 1.

All the bond distances and angles are as anticipated for this type of bonding.

In the structure of **1**, four *m*-toluidine molecules are protonated getting +1 charge, which play an important

role in the formation of the framework. There are many types of hydrogen bonds (Table S1 in Supplementary Information) (C—H ··· O, N—H ··· O and O—H ··· O) and the majority of them formed

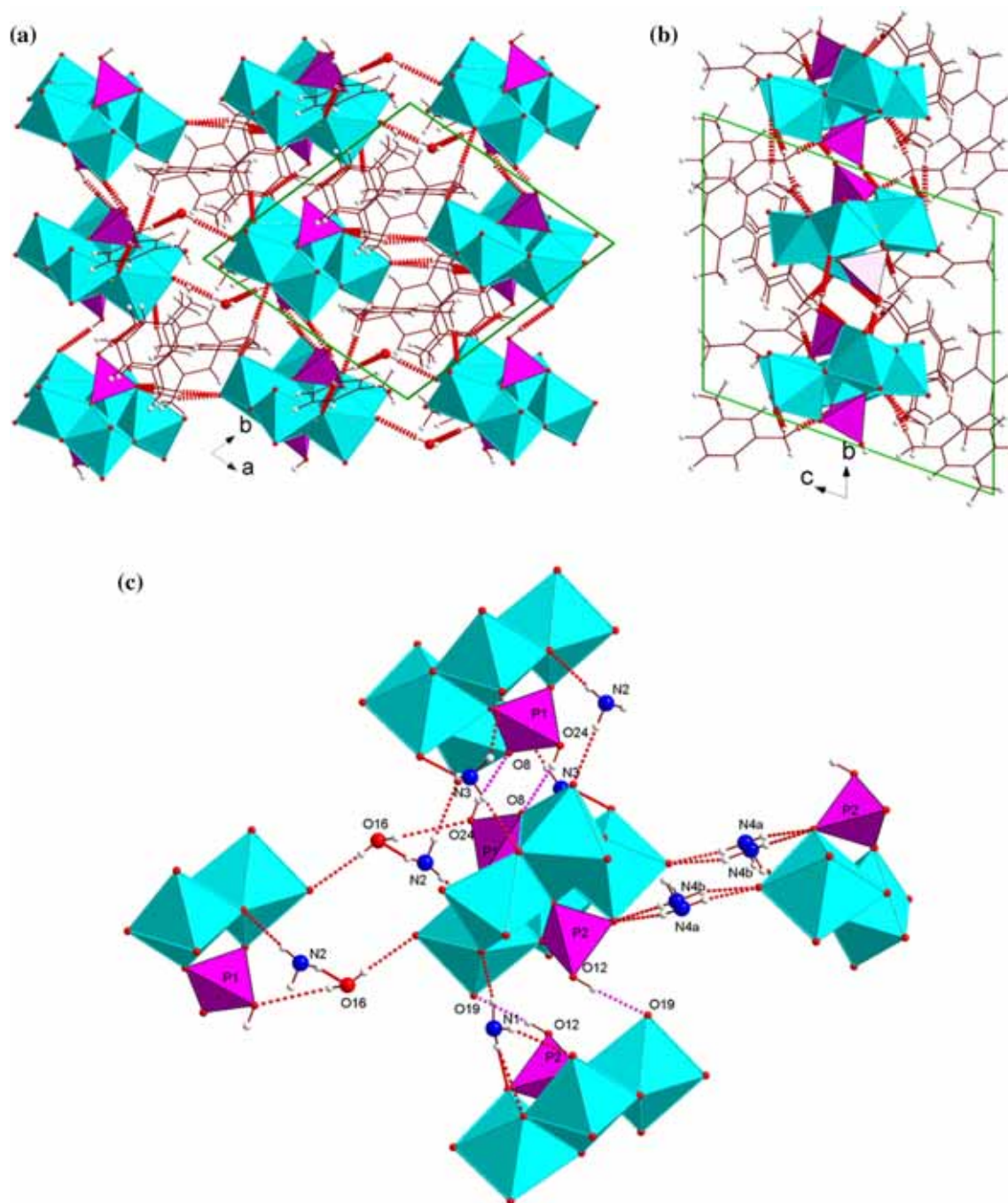


Figure 3. The O...O and N...O hydrogen bonds in **1** with the distance between hydrogen and acceptor below 2.1 Å and the D-H...A angle above 144°. Colour code: light blue polyhedral belong to Mo, violet polyhedral belong to P; red circle – oxygen, white circle – hydrogen, deep blue circle – nitrogen; read and pink dashed lines – hydrogen bonds; green thick line – unit cell edges. (a) View along *c* of a slab of molecules parallel with *ab* and connected with hydrogen bonds. (b) View along *a* showing that only weak C-H...O interactions which connect the parallel slabs. (c) Detailed view on hydrogen bonds. Pink dashed lines indicate direct connections between the clusters of polyanions [H₂P₂Mo₅O₂₃]⁴⁻ while red dashed lines distinguish indirect connections through NH₃ group or the lattice water.

between the terminal oxygen atoms of the diphosphopentamolybdate and the hydrogen atoms of the amine groups. The complex network of hydrogen bonds (Figure 3) makes the crystal structure of **1** more stable.

We notice that water molecules in the structure of **1** appear to have an imperative role in binding either organic-P₂Mo₅ or P₂Mo₅-P₂Mo₅ groups. As shown in the packing diagram in Figure 3, each water molecule

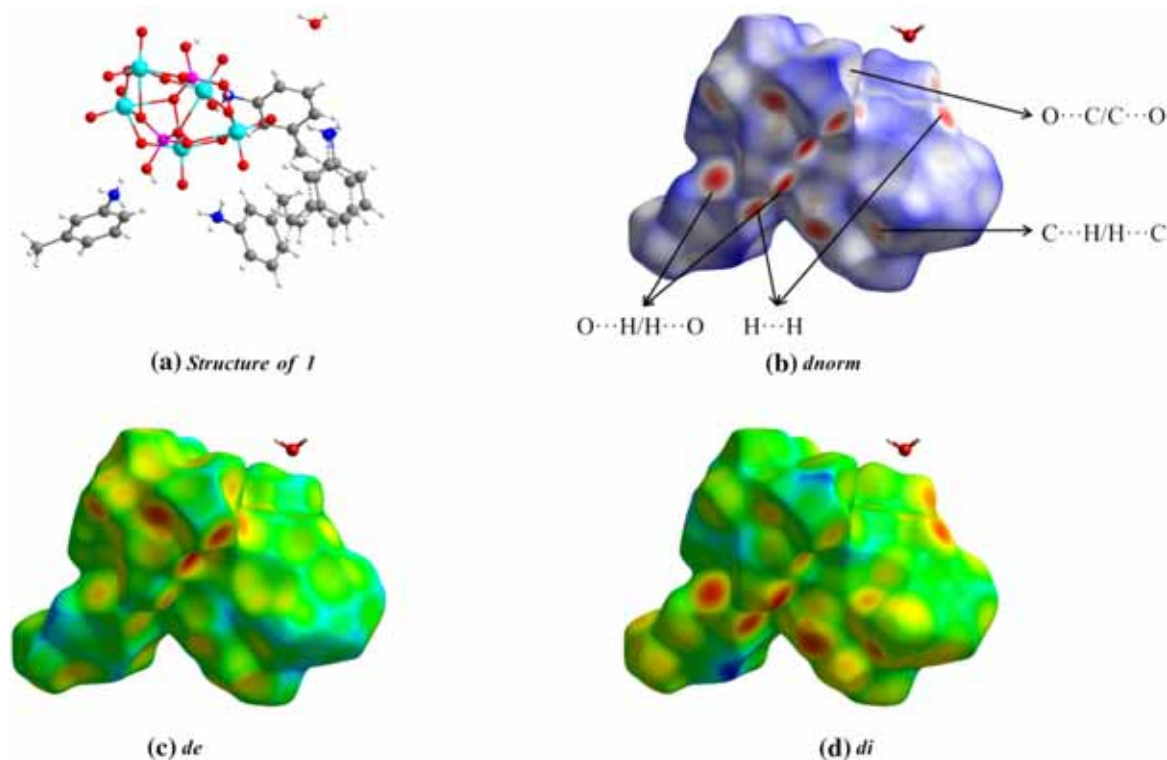


Figure 4. Hirshfeld surfaces mapped with $dnorm$ (mapped over a fixed color scale of -0.744 (red) to 1.488 (blue)), de and di of **1**.

connects two clusters and one protonated organic cation. So a 3D supramolecular structure is formed by alternate hydrogen bond interactions among water molecules and protonated *m*-toluidine.

3.2 Hirshfeld surface analysis

The Hirshfeld surfaces¹⁷ and fingerprint plots were generated based on the refined structure model of the title compound. This analysis helps to understand geometry and strength of intermolecular interactions by their visualization using appropriate color codes^{18–21} on the Hirshfeld surface, which is defined by points where the contribution of the molecule of interest to the overall electron density is equal to the input from all the other molecules. Two distances are calculated for each point on such isosurface: de and di , representing the distance from the point to the nearest nucleus external/internal to the surface. Another parameter, the normalized contact distance $dnorm$, is based on both de and di .²² Results of the Hirshfeld analysis are shown in Figure 4.

The 2D fingerprint plots (Figure 5) provide additional information about the intermolecular interactions. The major contributors to the crystal packing are interactions $O \cdots H/H \cdots O$ (53.4%) and $H \cdots H$ (30.5%), followed by $C \cdots H/H \cdots C$ (12.7%) and $O \cdots C/C \cdots O$ (2.4%). Remaining contacts are negligible.

3.3 Vibrational spectra

IR spectrum of **1** was measured at room temperature between 4000 and 400 cm^{-1} (Figure 6). Several bands in the range of 3500 – 2000 cm^{-1} is ascribed to O–H stretching of water molecules, and also to N–H and C–H stretching vibrations.²³ The frequencies between 1530 and 1340 cm^{-1} are attributed to the C–N and C–C stretching vibrations of the organic part.²⁴ Remaining bands between 1650 – 1100 cm^{-1} are associated with O–H bending of water molecules and N–H and C–H bending vibrations.^{7,25} The compound also provides bands in 1100 – 1000 cm^{-1} region assigned to $\nu(\text{P–O})$.²⁶ Bands at 919 , 886 , 783 , 677 , 632 , 528 , 512 and 434 cm^{-1} are attributed to $\nu(\text{Mo=O}_t)$ and $\nu(\text{Mo–O–Mo})$.^{26,27}

3.4 UV–Vis spectra

The UV spectrum of the title compound in the aqueous solution was performed in the range of 200 – 800 nm (Figure 7) and it reveals two absorption peaks at 219 and 263 nm . The peak at 219 nm is ascribed to the charge transfer absorption of $O_t \rightarrow \text{Mo}$ LMCT band, and the absorption peak at 263 nm is attributed to the charge transfer $O_{b,c} \rightarrow \text{Mo}$.^{28,29} Using the limit value of absorption (315 nm), the optical energy gap (E_g) was

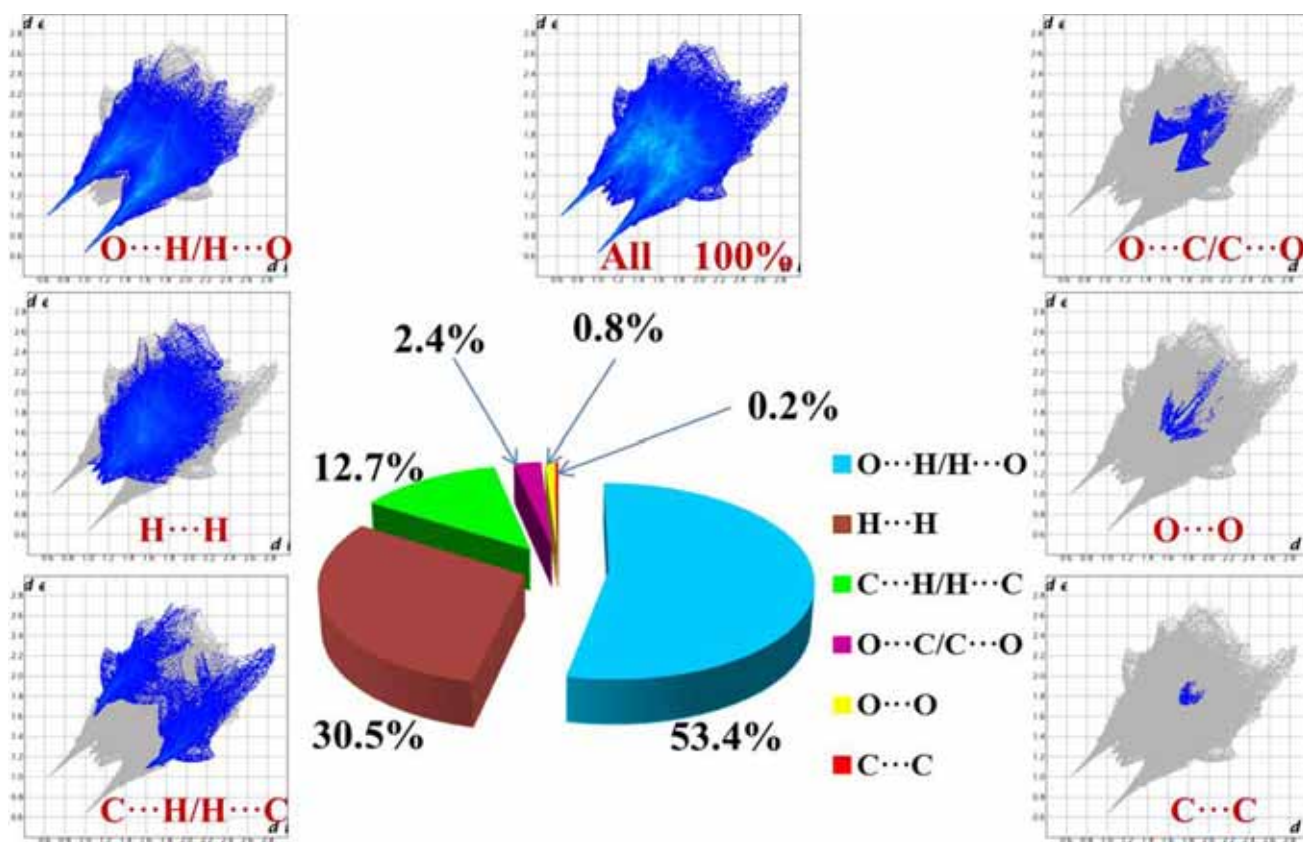


Figure 5. 2D fingerprint plots of 1.

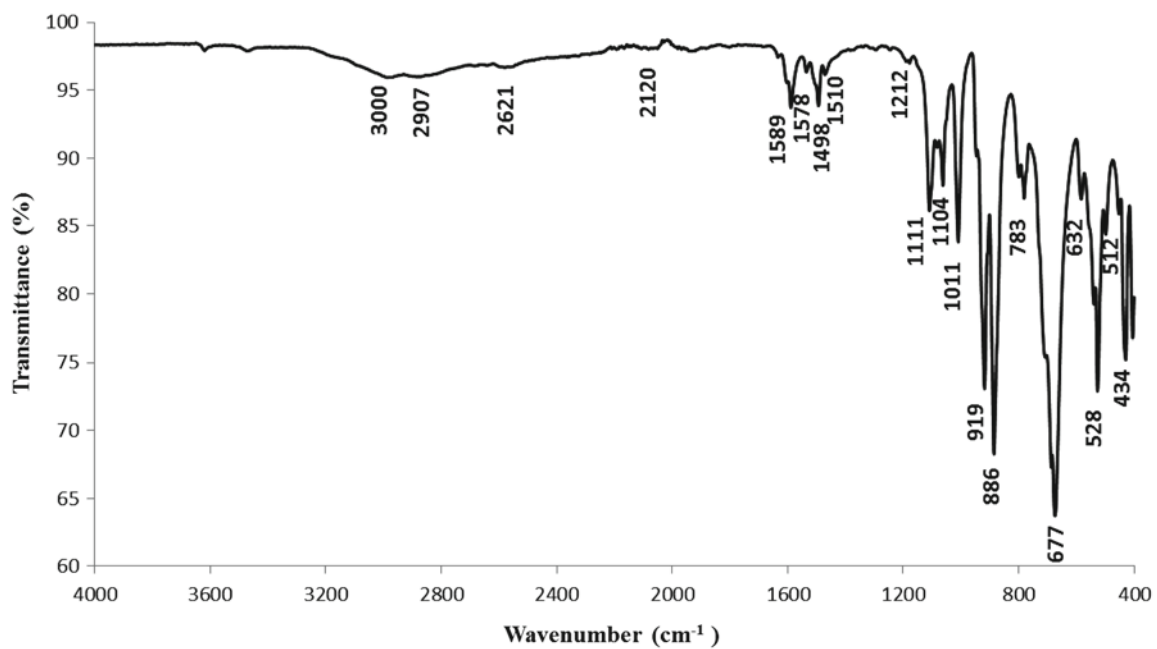


Figure 6. IR spectrum of compound 1.

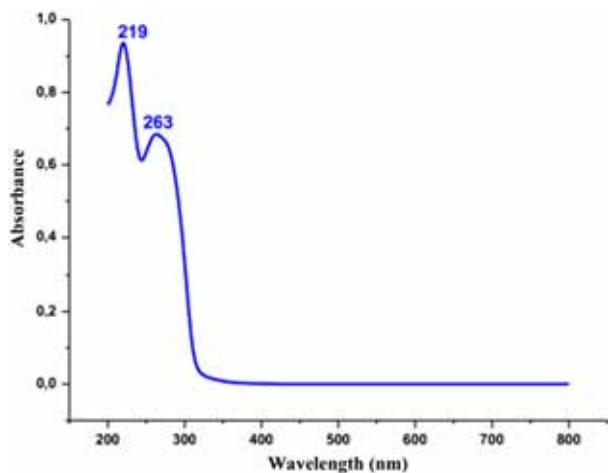


Figure 7. UV-Visible absorption spectrum of compound **1** ($C = 0.29 \times 10^{-3}$ mol/L, pathlength: 1 cm).

evaluated as 3.94 eV, allowing for classification of this compound as an insulator.

3.5 Frontier molecular orbital analysis (FMO)

HOMO, LUMO and the energy gap were calculated to establish the ability of **1** to absorb light, and to identify its chemical reactivity and kinetic stability.³⁰

The map of frontier molecular orbitals of the title molecule is illustrated in Figure 8. The HOMO and LUMO of the title compound are localized over part of oxygen atoms of $[\text{H}_2\text{P}_2\text{Mo}_5\text{O}_{23}]^{4-}$ anion and part of protonated *m*-toluidine. The energy values of HOMO and HOMO-1 are -6.69 and -6.80 eV, respectively. The energy values of LUMO and LUMO + 1 are -2.46 and -2.30 eV, respectively. From these values, we can calculate the energy gap of the title compound, as $\Delta E = 4.23$ eV for HOMO \rightarrow LUMO and $\Delta E = 4.5$ eV for HOMO-1 \rightarrow LUMO + 1.

3.6 Thermodynamic properties

In this work, the theoretical thermodynamic properties of the title compound were calculated to get information about the thermodynamic energies and their variations with temperature. The thermodynamic functions at 298.15 K and 1.00 atm, namely the zero point energy (ZPE), enthalpy (H°), heat capacity (C_V) and the entropy (S°), were calculated and values are listed in Table S2 (Supplementary Information). Also, the statistical thermochemical analyses were performed between 100 and 1000 K on the basis of vibrational analysis,

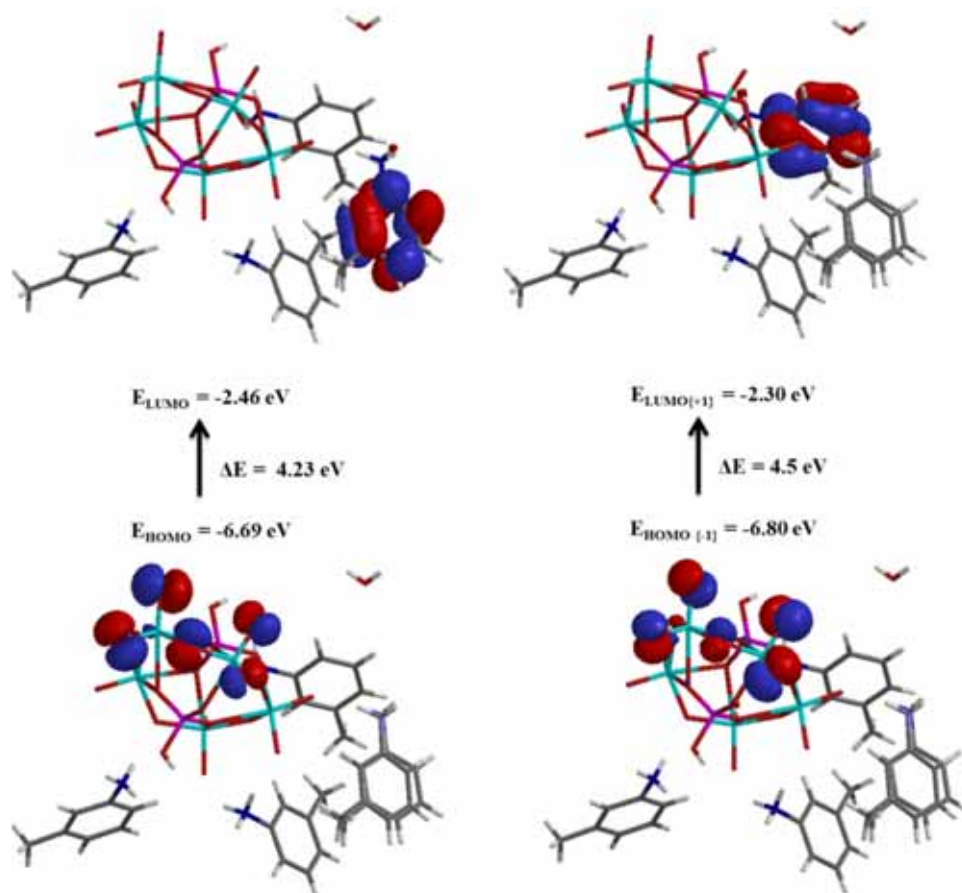


Figure 8. Frontier molecular orbital plots of **1**.

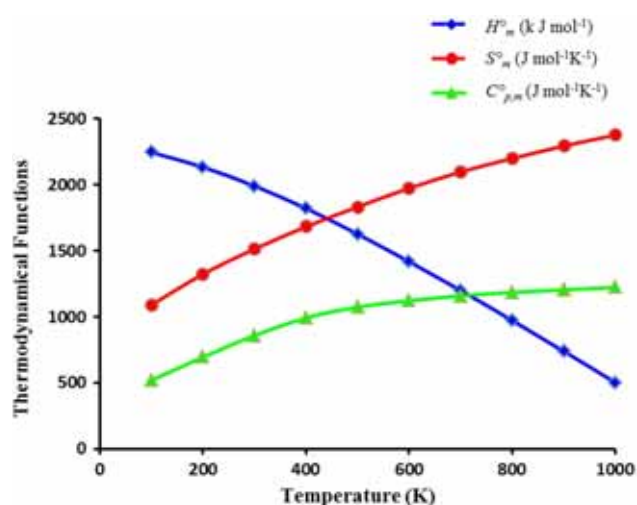


Figure 9. Variation in thermodynamic parameters with temperature for **1**.

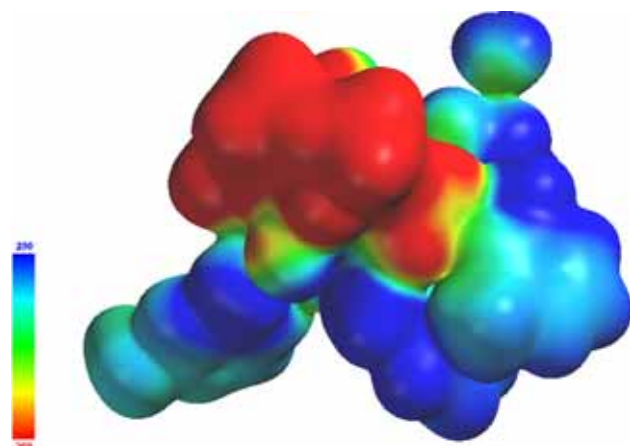


Figure 10. Molecular electrostatic potential (MEP) in the property range -200 to 200 kJ mol⁻¹.

with results listed in Table S3 (Supplementary Information). The correlation graphs are shown in Figure 9. The correlation equations between the thermodynamic parameters and temperature T are as follows:

$$H_m^\circ = 2316.67 - 0.526 T - 19.69 \times 10^{-4} T^2 \quad (R^2 = 0.99519) \quad (1)$$

$$S_m^\circ = 561.22 + 6.778 T - 148.41 \times 10^{-4} T^2 \quad (R^2 = 0.988345) \quad (2)$$

$$C_{p,m}^\circ = 291 + 2.58 T - 28.18 \times 10^{-4} T^2 \quad (R^2 = 0.926564) \quad (3)$$

3.7 Molecular electrostatic potential (MEP)

To visualize relative polarity and active sites of molecules, we can use molecular electrostatic potential, because it is very effective in the investigation of

the molecular structure to show the reactivity of the molecule and it provides a visual method to study the relative polarity.³¹ The 3D mapped surfaces of the MEP is shown in Figure 10. According to the MEP map, the different values at the surface are represented by different colours. The negative potential, red regions, are mainly localized over the terminal oxygen atoms of diphosphopentamolybdate anion. These regions are susceptible for electrophilic attack in the title compound. The regions around hydrogen atoms of water molecules and m-toluidine cation are the positive blue regions and they indicate possible sites for nucleophilic attack. The light green, yellow and orange regions in the MEP surfaces relate to a potential halfway between the two extremes in red and blue colours.

4. Conclusions

The title compound $(C_7H_{10}N)_4[H_2P_2Mo_5O_{23}] \cdot H_2O$ was synthesized and characterized by IR and UV spectroscopy, and its structure was solved by single crystal X-ray diffraction. The presence of the Mo, P, O, C and N atoms was confirmed by EDS analysis. The Hirshfeld surface analysis was performed to elucidate non-bonding interactions. Also, some theoretical properties of the title compound were studied.

Supporting Information (SI)

Tables S1–S3 are available as Supplementary Information at www.ias.ac.in/chemsci. CCDC1544336, contain the supplementary crystallographic data for **1**. These data can be obtained freely via http://www.ccdc.cam.ac.uk/data_request/cif, or by e-mailing to data_request@ccdc.cam.ac.uk or by contacting directly the Cambridge Crystallographic Data Centre (12 Union Road, Cambridge CB2 1EZ, UK. Fax: +44 1223 336033).

Acknowledgements

This work was supported by the Ministry of Higher Education and Scientific Research of Tunisia. The crystallographic part was supported by the project 15-12653S of the Czech Science Foundation using instruments of the ASTRA lab established within the Operation program Prague Competitiveness - Project CZ.2.16/3.1.00/24510.

References

- Tohomas J, Kannan K R and Ramanan A 2008 Nanostructured phosphomolybdates *J. Chem. Sci.* **120** 529
- Arumuganathan T, Siddikha A and Das S K 2017 'Ionic crystals' consisting of trinuclear macrocations and polyoxometalate anions exhibiting single crystal to single

- crystal transformation: breathing of crystals *J. Chem. Sci.* **129** 1121
- Li S, Li Z, Zhang J, Su Z, Qi S, Guo S and Tan X 2017 Polyoxometalate-based 3D porous framework with inorganic molecular nanocage units *J. Chem. Sci.* **129** 573
 - Hmida F, Ayed M, Ayed B and Haddad A 2015 Two new inorganic-organic hybrid materials based on inorganic cluster, $[X_2Mo_{18}O_{62}]^{6-}$ ($X = P, As$) *J. Chem. Sci.* **127** 1645
 - Miras HN, Yan J, Long D L and Cronin L 2012 Engineering polyoxometalates with emergent properties *Chem. Soc. Rev.* **41** 7403
 - Qu X, Xu L, Yang Y, Li F and Guo W 2011 Hydrothermal synthesis and crystal structure of $(H_2bpp)_3[Mo_5P_2O_{23}]H_2O$: a twofold interpenetrating 3D supramolecular architecture constructed of Strandberg-type polyoxometalate *Struct. Chem.* **22** 965
 - Ganesan S V and Natarajan S 2005 Hydrothermal synthesis and structure of $[(C_4N_2H_{12})_3][P_2Mo_5O_{23}] \cdot H_2O$ and $[(C_3N_2H_{12})_3][P_2Mo_5O_{23}] \cdot 4H_2O$ *J. Chem. Sci.* **117** 219
 - Liu H, Wang H, Niu D and Lu Z 2007 Microwave-Assisted Synthesis and Crystal Structure of Molybdophosphate Supramolecular Compound with 2-Aminopyridinium Cations *Synth. React. Inorg. Met. Org. Nano-Met. Chem.* **37** 103
 - Asnani M, Kumar D, Duaisamy T and Ramanan A 2012 Crystallization of organically templated phosphomolybdate cluster-based solids from aqueous solution *J. Chem. Sci.* **124** 1275
 - Palatinus L and Chapuis G 2007 SUPERFLIP - a computer program for the solution of crystal structures by charge flipping in arbitrary dimensions *J. Appl. Crystallogr.* **40** 786
 - Petricek V, Dusek M and Palatinus L 2014 Crystallographic Computing System JANA2006: General Features *Z. Kristallogr.* **229** 345
 - Brandenburg K and Putz H 2005 DIAMOND Version 3. Crystal Impact GbR, Postfach 1251, D-53002 Bonn, Germany
 - Spartan 14 2014 Wavefunction Inc. Irvine CA 92,612, USA
 - Spackman M A and McKinnon J J 2002 Fingerprinting intermolecular interactions in molecular crystals *CrystEngComm* **4** 378
 - Wolff S K, Grimwood D J, McKinnon J J, Turner M J, Jayatilaka D and Spackman M A 2012 CRYSTAL-EXPLORER 3.0 University of Western Australia, Perth
 - Jayatilaka D, Grimwood D J and Lee A 2005 TONTO A System for Computational Chemistry (Nedlands: The University of Western Australia)
 - Hirshfeld F L 1977 Bonded-atom fragments for describing molecular charge densities *Theor. Chim. Acta* **44** 129
 - Luo Y H, Mao Q X and Sun B W 2014 Two new complexes with 6-methylnicotinic acid ligand: Synthesis, crystal structure and Hirshfeld surfaces *Inorg. Chim. Acta* **412** 60
 - Luo Y H, Sun B W 2013 Pharmaceutical co-crystals of pyrazinecarboxamide (PZA) with various carboxylic acids: crystallography, Hirshfeld surfaces, and dissolution study *Cryst. Growth Des.* **13** 2098
 - Luo Y H, Xu Band Sun B W 2013 Investigation of supramolecular synthons of p-hydroxybenzoic acid (PHBA): Comparison of its hydrate, co-crystal and salt *J. Cryst. Growth* **374** 88
 - Desiraju G R and Gavezzotti A 1989 Crystal structures of polynuclear aromatic hydrocarbons Classification, rationalization and prediction from molecular structure. *Acta Crystallogr. Sec. B: Struct. Sci.* **45** 473
 - Prasad A A, Muthu K, Meenatchi V, Rajasekar M, Agilandeshwari R, Meena K, Manonmoni J V and Meenakshisundaram S P 2015 Optical, vibrational, NBO, first-order molecular hyperpolarizability and Hirshfeld surface analysis of a nonlinear optical chalcone *Spectrochim. Acta Part A: Mol. Biomol. Spect.* **140** 311
 - Ammari Y, Dhahri E, Rzaigui M, Hlil E K and Abid S 2016 Synthesis, structure and physical properties of an hybrid compound based on Strandberg type polyoxoanions and copper cations *J. Clust. Sci.* **27** 1213
 - He X, Zhang P, Song T Y, Mu Z C, Yu J H, Wang Y and Xu J N 2004 Hydrothermal synthesis and structure of a molybdenum(VI) phosphate cluster and a three dimensional cobalt molybdenum(V) phosphate *Polyhedron* **23** 2153
 - Wei C X, Chen J X, Huang Y B, Lan T Y, Li Z S, Zhang W J and Zhang Z C 2006 Syntheses, structures and properties of two molybdenum phosphates $[(H_2O)_8P_8Mo_{12}^{VI}CdO_{62}](C_4H_{14}N_3)_2]2C_4H_{13}N_3 \cdot 8H_2O$ and $[(H_2P_2Mo_5^{VI}O_{23})(C_4H_{14}N_3)(C_4H_{15}N_3)(H_3O)]3H_2O$ *J. Mol. Struct.* **798** 117
 - Ma Y, Lu Y, Wang E, Xu X, Guo Y, Bai X and Xu L 2006 Hydrothermal synthesis and crystal structure of a novel three-dimensional supramolecular network containing cyclic water hexamers: $[Co(en)_3]_4[P_2Mo_5O_{23}]_2 \cdot 9H_2O$ ($en = ethylenediamine$) *J. Mol. Struct.* **784** 18
 - Wang Y, Zhang L C, Zhu Z M, Li N, Deng A F and Zheng S Y 2011 Assembly of four copper(II)-2,2'-biimidazole complex-supported Strandberg-type phosphomolybdates *Transit. Met. Chem.* **36** 261
 - Nagazi I and Haddad A 2012 Synthesis, characterization and crystal structure of a novel Strandberg-type polyoxoselenomolybdate $Rb_4[Se_2Mo_5O_{21}] \cdot 2H_2O$ *Mat. Res. Bull.* **47** 356
 - Zhao J W, Li Y Y, Wang Y H, Shi D Y, Luo J and Chen L J 2013 A novel 2D phosphomolybdate hybrid $[Cu(En)(EnH)]_2[P_2Mo_5O_{23}] \cdot 3H_2O$ constructed from strandberg-type polyoxometalate units and copper-organic cation bridges *Rus. J. Coord. Chem.* **39** 519
 - Sharma S, Brahmachari G, Banerjee B, Nurjama K, Kumar A K, Srivastava A, Misra N, Pandey S K, Rajnikant and Gupta V K 2016 Synthesis, spectroscopic characterization and crystallographic behavior of a biologically relevant novel indole-fused heterocyclic compound — Experimental and theoretical (DFT) studies *J. Mol. Struct.* **1118** 344
 - Soria-Martínez R, Mendoza-Merono R and García-Granda S 2016 Synthesis, crystal structure, spectroscopic characterization and theoretical study of (2E)-N-phenyl-2-(pyridin-3-ylmethylidene)hydrazinecarboxamide *J. Mol. Struct.* **1105** 322